

Monte Carlo calculation of the energy response characteristics of a RadFET radiation detector

To cite this article: P Belicev *et al* 2010 *J. Phys.: Conf. Ser.* **238** 012030

View the [article online](#) for updates and enhancements.

Related content

- [In-house developed MOSFET dosimeter](#)
Dirk Verellen, Sven Van Vaerenbergh, Koen Tournel *et al.*
- [Monte Carlo simulation with PENELOPE to study MOSFET detectors](#)
M A Carvajal, S García-Pareja, D Guirado *et al.*
- [Performance characteristics of a microMOSFET as an in vivo dosimeter in radiation therapy](#)
R Ramaseshan, K S Kohli, T J Zhang *et al.*

Recent citations

- [S. Stankovic *et al*](#)

Monte Carlo Calculation of the Energy Response Characteristics of a RadFET Radiation Detector

P.Belicev², V.Spasic Jokic¹, S.Mayer³, M.Milosevic², R.Ilic², M.Pesic²

1 Faculty of Technical Sciences, University of Novi Sad, 2100 Novi Sad, Trg Dositeja Obradovica 6, Serbia

2 VINCA Institute of Nuclear Sciences, 11001 Belgrade, PB 522, Serbia

3 Paul Scherrer Institute, Villingen, Switzerland

E-mail: svesna@uns.ac.rs

Abstract. The Metal -Oxide Semiconductor Field-Effect-Transistor (MOSFET, RadFET) is frequently used as a sensor of ionizing radiation in nuclear-medicine, diagnostic-radiology, radiotherapy quality-assurance and in the nuclear and space industries. We focused our investigations on calculating the energy response of a p-type RadFET to low-energy photons in range from 12 keV to 2 MeV and on understanding the influence of uncertainties in the composition and geometry of the device in calculating the energy response function. All results were normalized to unit air kerma incident on the RadFET for incident photon energy of 1.1 MeV. The calculations of the energy response characteristics of a RadFET radiation detector were performed via Monte Carlo simulations using the MCNPX code and for a limited number of incident photon energies the FOTELP code was also used for the sake of comparison. The geometry of the RadFET was modeled as a simple stack of appropriate materials. Our goal was to obtain results with statistical uncertainties better than 1% (fulfilled in MCNPX calculations for all incident energies which resulted in simulations with $1 - 2 \times 10^9$ histories).

1. Introduction

The Metal-Oxide Semiconductor Field-Effect-Transistor (MOSFET) is frequently used as a sensor of ionizing radiation so called RadFET. RadFET has numerous clinical applications in nuclear-medicine, diagnostic-radiology and radiotherapy. Clinical applications in radiotherapy are significant and cover in-phantom measurements (build-up curves for high energy photon beams, interface dosimetry, small field output factors); in-vivo dosimetry (external beam entrance and exit doses and skin doses, Total Body Irradiation, Intensity Modulated Radiation Therapy, Image Guided Radiation Therapy, Intra Operative Radiation Therapy, brachytherapy) and in - vivo dosimetry for radiotherapy patients not in the treatment area, but in the peripheral regions. MOSFET is also often used in nuclear and space industry as well as in Power Pulse Technique (PPT) [1,2]. Advantages of RadFET are numerous but some of them have metrological significance as: very small active volume (very thin active area); small size of the packaged MOSFET; dual bias system in dual MOSFET eliminates most correction factors; instantaneous readouts (on-line dosimetry); waterproof; efficient in use; the post radiation signal is permanently stored and is dose rate independent; point dose measurements are possible; nonvolatility of the accumulated dose. Disadvantages lie in finite lifetime (≈ 100 Gy), in energy and temperature dependence and sensitivity changes with accumulated dose for unbiased MOSFETs. [3] The accuracy of the MOSFET detector depends on the dose applied to the detector, and it is lower for

small doses. Results for the MOSFET device show that the level of accuracy that can be achieved using 95% confidence interval half widths range from approximately 10–2.5% when the absorbed dose ranges from 2 cGy to 10 cGy. These values provided a lower uncertainty in measured dose.[1]

Basically, a MOSFET consists of a p-type silicon semiconductor substrate, a layer of insulating oxide, and a metal gate. MOSFET dosimeters are based on the measurement of the threshold voltage, which is a linear function of absorbed dose. Ionizing radiation penetrating the oxide generates charge that is permanently trapped, thus causing a change in threshold voltage. The integrated dose may be measured during or after irradiation. The direct dose reading from the gate-threshold voltage involves uncertainties from uncorrected systematics of accumulated-dose effects and angular dependence in dosimeter placement. The linearity and the angular dependence of the MOSFET detector are about ± 2 to 3% and $\pm 2.5\%$. Thus, the uncertainties of the MOSFET in photon dosimetry are rather large. Such uncertainties need to be quantitatively assessed in the commissioning process before clinical application. Metrological verification of RadFET is based on verification of the basic characteristics of the MOSFET dosimetry, such as: accuracy and precision, linearity, reproducibility, dose-rate effect, accumulated-dose effect, fading effect, angular dependence, energy dependence, accuracy in tissue maximum ratio, and total scatter factor measurements in order to assess the accuracy, reliability, and usefulness in clinical applications such as pinpoint absolute dosimetry for small fields. [3].

Energy dependence is generally a function of radiation beam quality (energy). Since the dosimetry systems are calibrated at a specified radiation beam quality (or qualities) and used over a much wider energy range, the variation of the response of a dosimetry system with radiation quality (called energy dependence) requires correction. Ideally, the energy response should be flat (i.e. the system calibration should be independent of energy over a certain range of radiation qualities). In reality, the energy correction has to be included in the determination of the quantity for most measurement situations. In radiotherapy, for example, the quantity of interest is the dose to water (or to tissue). As no dosimeter is water or tissue equivalent for all radiation beam qualities, the energy dependence is an important characteristic of a dosimetry system.

The application of the MOSFET as detectors or device components requires investigation of their characteristics in the radiation fields. Limitations in measurement of MOSFET detector characteristics are successfully overcome using Monte Carlo program for simulation of the radiation transport through the detector structure. Small photon beams present numerous difficulties in physical dose measurement. As an alternative to benchmarking, many research groups have shown that the Monte Carlo method is capable of accurately predicting standard dosimetric parameters as well as dose in regions where electronic equilibrium is lacking. Small beams are perturbed by tissue heterogeneities in a manner that conventional methods are unable to predict. The Monte Carlo model of simulation of the dose response of a MOSFET dosimeter is developed because a experimentally measure the detailed dosimeter response is hardly. However, in this case assumed charged particle equilibrium, which did not exist in the sensitive volume of the dosimeter. Therefore their model failed to calculate the actual dose, and the outputs were regarded as only a first-order approximation at best. [2]

2. Materials and methods

We focused our investigations on calculating the energy response of a p-type RadFET to low-energy photons and on understanding the influence of uncertainties in the composition and geometry of the device in calculating the energy response function. This investigations were the part of CONRAD intercomparisons. Further, under the majority of conditions, the threshold-voltage shift is directly proportional to the energy deposited in the oxide-layer and thence to the absorbed dose, so we can effectively calculate the response of the dosimeter by correctly calculating the deposited energy in the oxide-layers. Chosen energy range was from 12 keV to 2 MeV for photon sources considered as monoenergetic, but all results were normalized to unit air kerma incident on the RadFET for incident photon energy of approximately ^{60}Co energy of 1.1 MeV. An additional energy of 662 keV was introduced. The calculations of the energy response characteristics of a RadFET radiation detector were performed via Monte Carlo simulations using the MCNPX code [4]. For a limited number of

incident photon energies and only for the ‘capped’ configuration of the device, the FOTELP code [2,5] was also used for the sake of comparison. Energy response function of the RadFET should be calculated, as well as the influence of its kovar cap be investigated.

FOTELP: Physical rigor is maximized by employing the best available cross sections [6] and high speed routines for random values sampling from their distributions, and the most complete physical model for describing the transport and production of the photon/electron/positron cascade from 100.0 MeV down to 1.0 keV. The code is developed for photon, electron and positron numerical experiments by Monte Carlo techniques for dosimetry and radiation damage. For the photon history, the trajectory is generated by following it from scattering to scattering using corresponding inverse distribution between collision, types of target, types of collisions, types of secondaries, their energies and scattering angles. Photon interactions are photoelectric absorption, incoherent scattering, pair production, and coherent scattering. The histories of secondary photons include bremsstrahlung and positronelectron annihilation radiation. The condensed history Monte Carlo method is used for the electron and positron transport simulation. During a history the particles lose energy in collisions, and the secondary particles are generated on the step according to the probabilities for their occurrence. Electron (positron) energy loss is through inelastic electron-electron (e-,e-) and positron-electron (e+,e-) collisions and bremsstrahlung generation. The fluctuation of energy loss (straggling) is included according to the Landau's or Blunk-Westphal distributions. The secondary electrons, which follow history of particles, include knock-on, pair production, Compton and photoelectric electrons. The secondary positrons are included too. With atomic data, the electron and positron Monte Carlo simulation is broadened to treat atomic ion relaxation after photoeffect and impact ionization. [2,7]

The geometry of the RadFET was modeled as a simple stack of appropriate materials. Our goal was to obtain results with statistical uncertainties better than 1% (fulfilled in MCNPX calculations for all incident energies except 1.1 and 1.5 MeV) which resulted in simulations with $1 - 2 \times 10^9$ histories.

Since the thicknesses of some material zones within the device are very small (below $1 \mu\text{m}$, typically about 500 nm) our primary concern was to investigate if the condensed macro steps for the generated electrons are small enough in order not to spoil the correct energy deposition in the layers. The performed preliminary calculations with different values of the *estep* MCNPX's parameter proved that its default value is sufficiently good (see Fig. 1). However, in order to be on the safe side, in all calculations and for all material zones we adopted the value *estep* = 15.

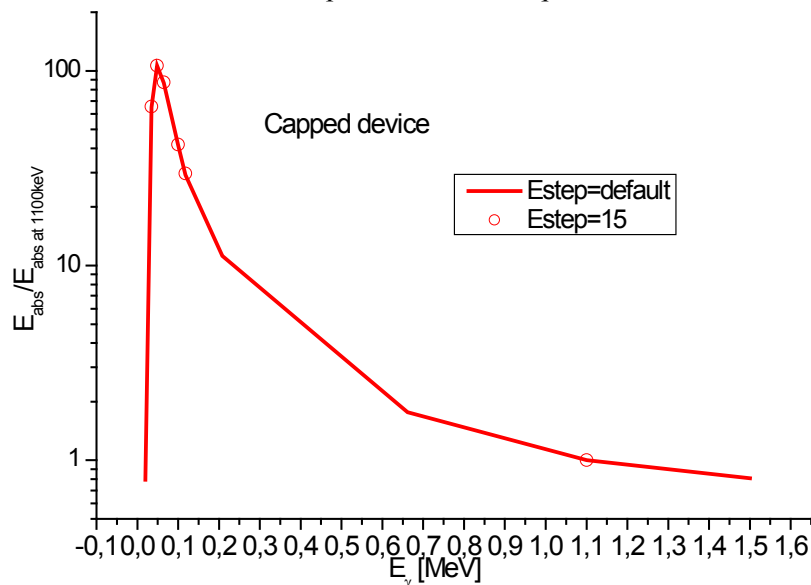


Figure 1. Influence of the *estep* MCNPX's parameter on energy deposition in layer 5.

For normalization of the obtained results to unit air kerma we used ICRU 57 [8] data of fluence to air kerma conversion factors ($F_{\phi \rightarrow k}$). The values for E_γ from ICRU 57 do not coincide with all energies required in the problem. An appropriate interpolation between the tabulated values was performed (Figure 2).

Table 1. Fluence to air kerma conversion factors $F_{\phi \rightarrow k}$ in [$\text{pGy} \times \text{cm}^2$].
 Photon energy E_γ is in [keV] (ICRU 57).

E_γ	$F_{\phi \rightarrow k}$	E_γ	$F_{\phi \rightarrow k}$	E_γ	$F_{\phi \rightarrow k}$	E_γ	$F_{\phi \rightarrow k}$	E_γ	$F_{\phi \rightarrow k}$
10	7.43	50	0.323	200	0.856	800	3.69	4000	12.1
15	3.12	60	0.289	300	1.38	1000	4.47	5000	14.1
20	1.68	80	0.307	400	1.89	1500	6.14	6000	16.1
30	0.721	100	0.371	500	2.38	2000	7.55	8000	20.1
40	0.429	150	0.599	600	2.84	3000	9.96	10000	24.0

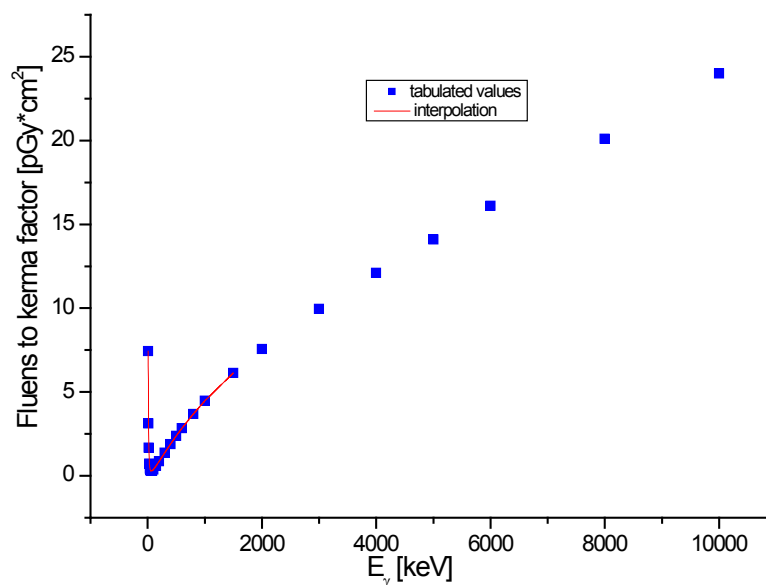


Figure 2. Interpolation of fluence to air kerma conversion factors $F_{\phi \rightarrow k}$ based on values from Table 1.

3. Results and discussion

3.1. The response function for capped device

The response function for the capped device has been calculated using MCNPX and FOTELP codes. The reason for using both codes is twofold: to check the correctness of the RadFET model implementation (geometry, materials, input parameters etc.) and to compare the results obtained. Since the use of FOTELP was restricted to a single PC resource (the cluster option was not available), this code was used only for the capped device calculations. The response function of the capped configuration of RadFET in the required energy range is presented in Fig. 3. and in Tables 2 and 3.

The results show that the RadFET capped configuration has a response function with local maximum for the incident photon energy of about 35 keV, which make it convenient in X-ray dosimetry.

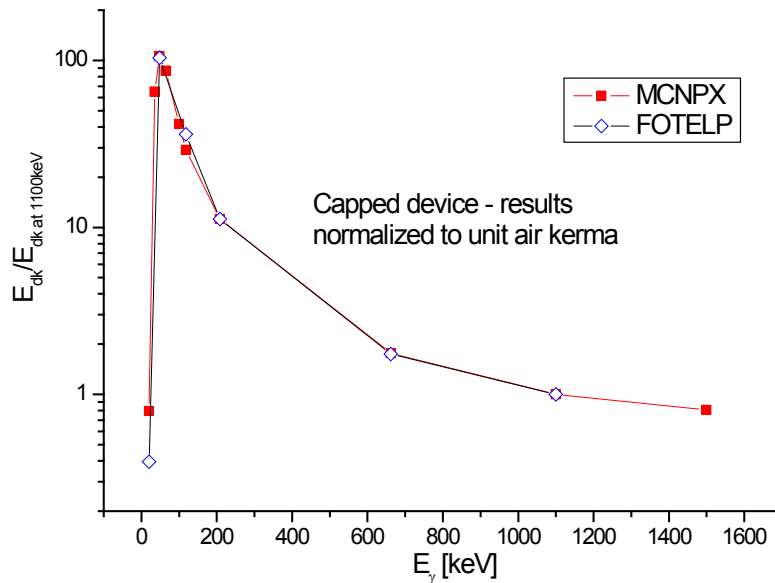


Figure 3. Response function of the RadFET capped configuration in the required energy range, calculated by MCNPX and FOTELP code.

Table 2. Deposited energy in region 5 of the capped device obtained by MCNPX (E_d - deposited energy per incident photon; $(E_{dk}/E_{1.1\text{MeV}}) - E_d$ value normalized to unit air kerma, relative to value for incident photon energy of 1.1 MeV). Number of histories 2×10^9 .

E_γ [keV]	20	35	48	65	100	118	208	662	1100	1500
$E_d \times 10^2$ [eV]	1.88	52.72	51.46	35.86	21.71	18.609	14.16	7.716	6.762	6.979
\pm [%]	± 1.3	± 0.2	± 0.23	± 0.27	± 0.35	± 0.38	± 0.44	± 0.68	± 1.15	± 1.26
$E_{dk}/E_{1.1\text{MeV}}$	0.7957	65.14	106.2	86.79	41.56	29.18	11.21	1.7663	1.00	0.8074

Table 3. Deposited energy in region 5 of the capped device obtained by FOTELP (E_d - deposited energy per incident photon; $(E_{dk}/E_{1.1\text{MeV}}) - E_d$ value normalized to unit air kerma, relative to value for incident photon energy of 1.1 MeV). Number of histories 1×10^9 .

E_γ [keV]	20	35	48	65	100	118	208	662	1100	1500
$E_d \times 10^2$ [eV]	0.857	-	46.0	-	-	21.1	13.0	6.99	6.20	-
\pm [%]	± 6.8	-	± 0.43	-	-	± 1.01	± 1.32	± 1.28	± 1.3	-
$E_{dk}/E_{1.1\text{MeV}}$	0.395	-	103.6	-	-	36.08	11.2	1.75	1.00	-

The results show that the RadFET capped configuration has a response function with local maximum for the incident photon energy of about 35 keV, which make it convenient in X-ray dosimetry.

3.2. The response function for uncapped device

By omitting the first zone in the RadFET capped configuration (the second one contains vacuum) one comes to the uncapped configuration, characterized by absence of the cover cap. In this case, the response function has been calculated using only the MCNPX code. The results are presented in Fig. 4 as well as in Table 4.

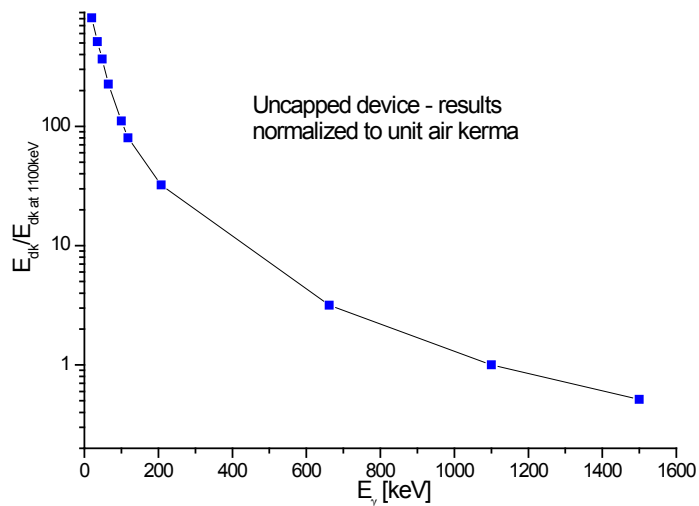


Figure 4. Response function of the RadFET uncapped configuration in the required energy range

Table 4. Deposited energy in region 5 of the uncapped device (E_d - deposited energy per incident photon; $(E_{dk}/E_{1.1\text{MeV}}) - E_d$ value normalized to unit air kerma, relative to value for incident photon energy of 1.1 MeV). Number of histories 1×10^9 .

E_γ [keV]	20	35	48	65	100	118	208	662	1100	1500
$E_d \times 10^2$ [eV]	519.66	112.2	47.99	25.25	15.65	13.85	11.04	3.749	1.83	1.20
\pm [%]	± 0.08	± 0.16	± 0.24	± 0.32	± 0.42	± 0.45	± 0.50	± 0.89	± 1.41	± 1.65
$E_{dk}/E_{1.1\text{MeV}}$	811.15	511.9	365.6	225.6	110.6	80.14	32.23	3.168	1.00	0.513

In case of the RadFET uncapped configuration, the response function does not have a local maximum. Maximum continually decreases against the incident photon energy, having maximal value at 20 keV.

References

- [1] Martin J, Butsona B, Cheunga T and Yu KN. 2005 Peripheral dose measurement with a MOSFET detector *Applied Radiation and Isotopes* **62** 631–34
- [2] Stankovic J, Ilic RD, Osmokrovic P, Loncar B and Vasic A 2006 Computer Simulation of Gamma Irradiation Energy Deposition in MOSFET Dosimeters, *IEEE Transactions On Plasma Science* **34** (5) 1715- 18
- [3] Ryosuke K, Hirano E, Nishio T, Miyagishi T, Goka T, Kawashima M and Ogino T 2008 Dosimetric evaluation of a MOSFET detector for clinical application in photon therapy *Radiol Phys Technol* **1** 55-61
- [4] Pelowitz DB *MCNPX User's Manual, Version 2.5.0* 2005 (Los Alamos: LA-CP-05-0369)

- [5] Ilic RD 2003 FOTELP-2K3 Photon, Electron and Positron Monte Carlo Transport Simulation, NEA Data Bank, IAEA 1388
- [6] Berger M J and Seltzer S M 1999 XCOM Photon Cross Sections, Version 3.1, NISTIR <http://physics.nist.gov/PhysRefData/Xcom/Text/intro.htm>
- [7] Ilic RD 2004 FOTELP-2K3: Photons, Electrons and Positrons Transport in 3D by Monte Carlo Techniques, OECD NEA Data bank , *IAEA-1388* <http://www.nea.fr/dprog/>
- [8] ICRU Report 57 1998 *Conversion Coefficients for use in Radiological Protection against External Radiation* (Bethesda, MD: ICRU)